Research Square

Preprints are preliminary reports that have not undergone peer review.
They should not be considered conclusive, used to inform clinical practice,
or referenced by the media as validated information.

Coupled atmospheric moisture and trade networks reveal a concentration of global freshwater risk in a handful of countries

Simon Fahrländer

Simon.Fahrlaender@pik-potsdam.de

Potsdam Institute for Climate Impact Research https://orcid.org/0009-0004-8377-530X

Romi Lotcheris

Stockholm University https://orcid.org/0000-0002-9784-1978

Lauren Andersen

Potsdam Institute for Climate Impact Research (PIK) https://orcid.org/0000-0003-3080-0503

Dieter Gerten

Potsdam Institute for Climate Impact Research https://orcid.org/0000-0002-6214-6991

Jonathan Donges

Potsdam Institute for Climate Impact Research

Marta Tuninetti

Polytechnic University of Turin https://orcid.org/0000-0003-2619-8783

Arie Staal

Utrecht University https://orcid.org/0000-0001-5409-1436

Lan Wang-Erlandsson

Stockholm University https://orcid.org/0000-0002-7739-5069

Johan Rockström

Potsdam Institute for Climate Impact Research https://orcid.org/0000-0001-8988-2983

Nico Wunderling

Center for Critical Computational Studies (C3S), Goethe University Frankfurt

Article

Keywords: Moisture recycling, VWT, water networks, telecoupling, water security

Posted Date: June 23rd, 2026

DOI: https://doi.org/10.21203/rs.3.rs-9932461/v1

License: This work is licensed under a Creative Commons Attribution 4.0 International License.
Read Full License

Additional Declarations: There is **NO** Competing Interest.

Coupled atmospheric moisture and trade networks reveal a concentration of global freshwater risk in a handful of countries

Simon F. Fahrländer[1,2*], Romi Lotcheris[3,4], Lauren S. Andersen[1], Dieter Gerten[1,5], Jonathan F. Donges[1,3,6], Marta Tuninetti[7], Arie Staal[8], Lan Wang-Erlandsson[1,3,4], Johan Rockström[1,2,3], Nico Wunderling[1,9,10]

[1*]Potsdam Institute for Climate Impact Research (PIK), Member of the Leibniz Association, P.O. Box 601203, 14473 Potsdam, Potsdam, Germany.
[2]Institute for Environmental Science and Geography, University of Potsdam, Potsdam, Germany.
[3]Stockholm Resilience Centre, Stockholm University, Stockholm, Sweden.
[4]Bolin Centre for Climate Research, Stockholm University, Stockholm, Sweden.
[5]Geography Department and IRI THESys, Humboldt-Universität zu Berlin, Berlin, Germany.
[6]Integrative Earth System Science, Max Planck Institute of Geoanthropology, Jena, Germany.
[7]Department of Environment, Land and Infrastructure Engineering, Politecnico di Torino, Turin, Italy.
[8]Copernicus Institute of Sustainable Development, Utrecht University, Utrecht, The Netherlands.
[9]Center for Critical Computational Studies (C3S), Goethe University Frankfurt, Frankfurt am Main, Germany.
[10]Senckenberg Research Institute and Natural History Museum, Member of the Leibniz Association, Frankfurt am Main, Germany.

*Corresponding author(s). E-mail(s): simon.fahrlaender@pik-potsdam.de;

Abstract

Atmospheric moisture flows transport $\sim \mathbf{26,000}\boldsymbol{km^3}$ of water across national boundaries annually, an order of magnitude larger than the $\sim \mathbf{1,700}\boldsymbol{km^3}$ of virtual water embedded in globally traded crop commodities. These flows are interrelated: atmospheric moisture sustains the agricultural production (and water use) that drives virtual water trade (VWT). However, the combined water dependencies from their interaction remain poorly understood. Here, we couple a global country-to-country atmospheric moisture network with a VWT network to assess their joint interactions across moisture sources, mediating countries, and trade sinks. We find that lower-income countries tend to act as net moisture sources while higher-income nations are net sinks of virtual water ($\boldsymbol{r} = 0.42$, $\boldsymbol{p} < 0.001$). A small set of countries, notably Argentina, the USA, and Ukraine, disproportionately link atmospheric moisture fluxes to agricultural trade, and their disruption would propagate losses across the same import-dependent countries. These coupled dependencies are increasingly critical for water resilience as climate change destabilises the hydrological cycle and geopolitical tensions render global supply chains more fragile.

Keywords: Moisture recycling, VWT, water networks, telecoupling, water security

Main

Moisture recycling processes, through which terrestrial evaporation in one region contributes to precipitation in another, have increasingly been recognised as important for rainfall-dependent agricultural production and ecosystem function [1–4]. Around half of all terrestrial precipitation originates from terrestrial evaporation [5, 6], making cross-border atmospheric moisture flows (AMF) a critical component of regional water availability. Virtual water trade (VWT), in turn, describes the freshwater consumed during production that is then "virtually" transferred via traded commodities to consumption places [7–9]. Both the atmospheric and the virtual water flow networks are increasingly impacted by human-induced pressures. AMF are directly affected by land-use change and climate change, which alter terrestrial evaporation and moisture recycling with consequences for precipitation-dependent production in downwind countries [1, 10, 11]. VWT is an entirely human-driven redistribution of embedded freshwater in traded commodities [7, 12], and it is altered by socio-economic and geopolitical modifications (e.g., trade agreements, prices), and by changes in the agricultural practices and water use that modify the embedded water content of traded commodities. Because a substantial share of staple crops and animal feed is produced in a few breadbasket regions (e.g., Ukraine and Argentina) and redistributed through trade, disruptions via drought, irrigation deficits, export restrictions, or conflict in exporting regions can propagate across borders [13, 14]. Export-driven water use can ease pressure in importing regions but also heighten international dependence and water stress in source areas [8]. This can undermine food security in import-dependent countries [14]. Each network operates across different spatial and temporal scales, governed by different mechanisms of water transport,

yet both link distant regions through trans-boundary dependencies. We refer to these dependencies as telecoupled moisture–trade pathways, in which atmospheric moisture teleconnections shape precipitation-dependent production, and trade transmits that dependence to distant consumers.

Recent research has shown that AMF between countries vary systematically with geography and climate: small landlocked nations tend to be highly dependent on external moisture sources, large countries are often more self-sufficient, and arid coastal states rely predominantly on oceanic evaporation [15, 16]. Cross-country AMF patterns reveal distinct typologies of interdependence, including bilateral exchange, dominant source regions which supply a large share of a downwind region's precipitation, cascading flows where moisture successively passes through multiple regions, and multilateral exchange networks [15], highlighting the need for a network-based systems approach [16]. VWT networks similarly are shaped by geography as well as political and economic patterns, including major trade hubs, asymmetric flows, and regions vulnerable to disruption [8, 17].

Freshwater distribution is increasingly shaped by telecoupled interactions in which biophysical and socio-economic flows connect distant places, such that changes in one network can alter exposure in the other [2, 18, 19]. Examining VWT alongside AMF in a coupled multilayer network framework offers new insights into how bio-physical and socio-economic systems interact to shape global freshwater patterns of redistribution and interdependence and resulting water resilience [8, 20]. Such network approaches have been useful in studying interdependencies and flow arrangements in Earth system processes, including characterising continental moisture recycling hubs [21, 22] and identifying global teleconnections in extreme-rainfall patterns [23]. While previous work has examined the effects of VWT on water stocks [24, 25] and on broader water-energy-food nexus dynamics [26], research explicitly linking the combined network effects of atmospheric moisture and VWT remains limited.

This study aims to investigate the roles of countries in freshwater dependence as a function of their position and centrality in the global coupled networks of AMF and VWT. This is done by applying complex network analysis to a novel reconciled dataset of bilateral AMF [16] and bilateral VWT [27]. Network nodes are represented by countries, as they constitute a critical jurisdictional unit for water governance and constitute the scale at which flow data are available [15, 28, 29]. By coupling these two cross-border freshwater networks (Fig. 1a,b), we identify feed-forward triples of the form $a \rightarrow b \rightarrow c$ (Fig. 1c): an atmospheric link $a \rightarrow b$ represents terrestrial evaporation in country a contributing to precipitation in country b, while a trade link $b \rightarrow c$ represents virtual-water exports from b to c. Together, these feed-forward paths define potential telecouplings in which moisture conditions in a shape consumption in c through production, water use, and export in b (see Methods (10)). As such, the analysis captures national water interdependencies across three dimensions: we explore how countries function as *sources* of downwind moisture embedded in trade (Fig. 1d),

as *mediators* linking atmospheric moisture to virtual water exports (Fig. 1e), and how they depend on distant water sources (Fig. 1f).

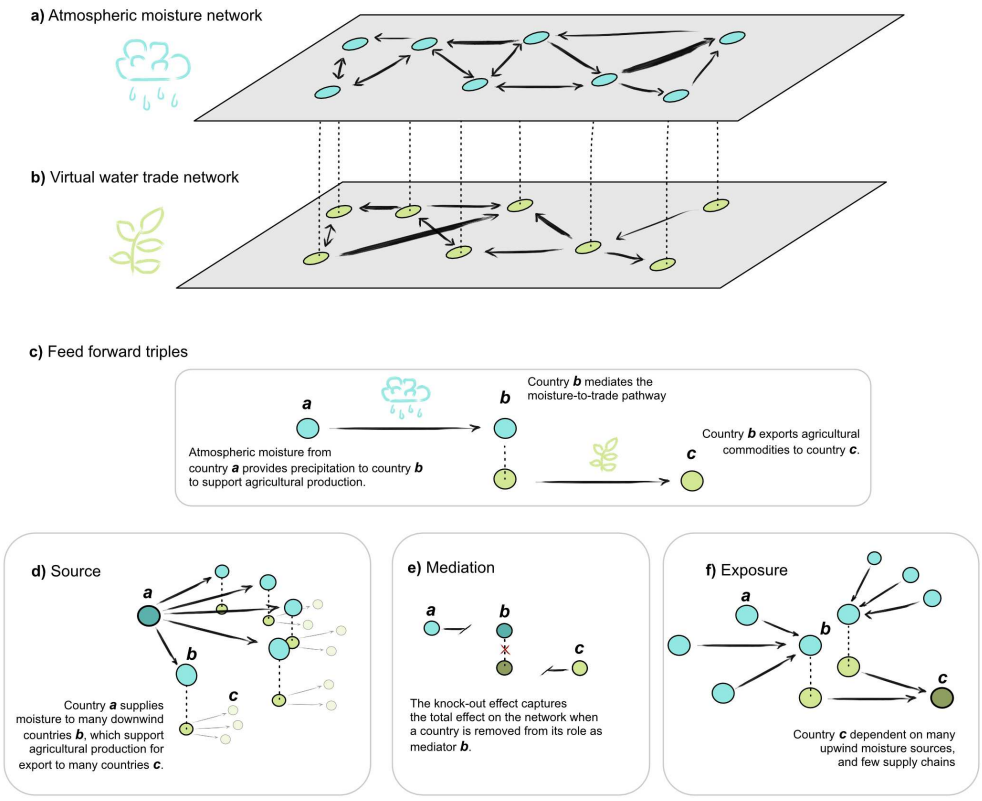


Fig. 1 Coupled atmospheric moisture transport and VWT networks. **(a)** Atmospheric moisture network consisting of weighted flows of terrestrial evaporation to precipitation among countries. **(b)** VWT network consisting of the volume of water embedded in traded agricultural goods among countries. **(c)** Conceptualisation of the *feed-forward triples* ($a \rightarrow b \rightarrow c$). The connection from country a to b is the atmospheric flow of water, which evaporates in a and rains down in b. Subsequently, the connection from country b to country c is provided by the VWT network, where products grown in b are traded to c. **(d)** Illustrative example of a country that acts as a large *source* in the network, by supplying moisture to many downwind countries, which use the moisture for agricultural production and export to many importing countries. **(e)** Illustrative example of a country's *mediation capacity*, quantified as the volume of VWT structurally attributable to upwind atmospheric moisture that passes through a single mediator country in the coupled network. **(f)** Illustrative example of a country that may have a high *exposure* based on the network structure, by importing commodities from several countries that, in turn, receive moisture from many others.

Results

Flow strength in the individual networks

Individually, both networks are highly concentrated in a few countries, yet organised according to distinct underlying logics (Fig. 2). Despite transferring considerably less water across borders than atmospheric flows ($\sim 26,000$ vs $\sim 1,700 km^3 yr^{-1}$), VWT is unconstrained by geography and can link producers and consumers across intercontinental distances. The atmospheric moisture network (Fig. 2a) is dominated by large tropical and continental countries, including Brazil, China, the Democratic Republic of the Congo (DRC), Russia, the USA, Canada, and Peru, where areal extent, terrestrial evaporation, and geographic position determine flow strength, i.e. the volume of water transferred between countries along network links. Moisture recycling is geographically constrained, operating primarily within regional and continental boundaries shaped by atmospheric circulation, resulting in clearly separated regional clusters. The VWT network (Fig. 2b), by contrast, is globally connected, and reflects commodity flows driven by agricultural output and trade capacity. The USA, China, Brazil, Indonesia, and Argentina dominate by total flow volume, alongside smaller re-exporting economies such as the Netherlands, Germany, Malaysia, and France. The two networks share a handful of dominant nodes but diverge considerably beyond them, with countries such as the DRC, Peru, and Bolivia providing significant atmospheric moisture sources, yet barely contributing to the VWT network.

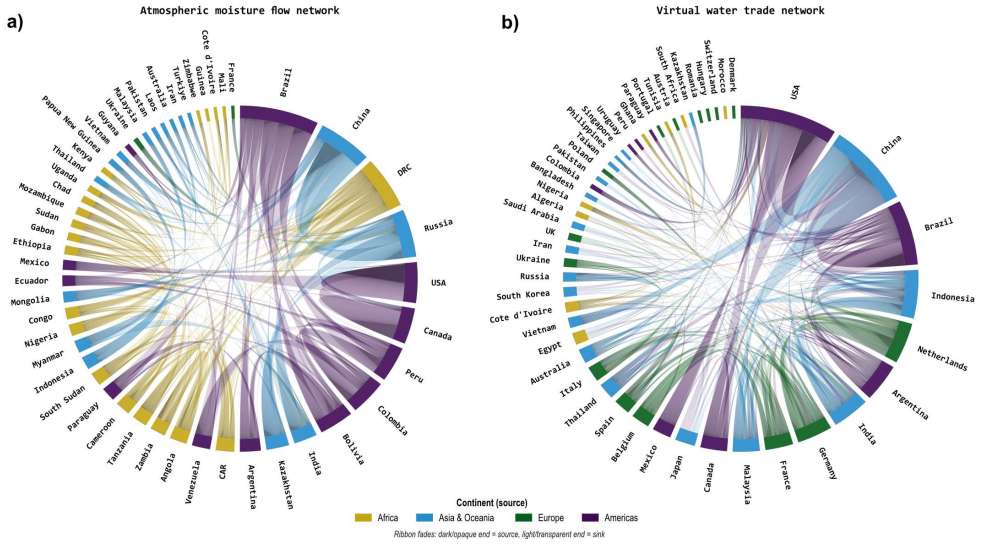


Fig. 2 Top 50 countries by total flow strength in the AMF (a) and VWT (b) networks. Nodes are arranged clockwise in descending order of total flow strength, with width proportional to a country's combined incoming and outgoing flow volume. Directed water flows (m^3) between country pairs that are at or above the 90th percentile of flows in each network are shown. Nodes are coloured by continent.

Diverging structural roles in the coupled network

Each country is assigned a structural role in the network, which is determined by how its atmospheric moisture contributions compare to the moisture-attributed virtual water it receives through trade via the coupled atmosphere–trade network. To quantify these roles, we extract feed-forward triples ($a \to b \to c$) from the tripartite network structure shown in Fig. 1. For each triple, the virtual water flow from mediator b to destination c is weighted by the fraction of b's precipitation originating from moisture source a, representing the volume of c's imports traceable to terrestrial evaporation in a, i.e. moisture-attributed trade flows. Aggregating across all triples yields a net position for each country, either as a source of moisture that sustains trade elsewhere, or as a sink of trade flows attributable to foreign moisture. We capture this by introducing an asymmetry index ranging from -1 to $+1$, with zero denoting balanced participation (10). A value of -1 indicates a country functions purely as an atmospheric moisture source, contributing moisture to downwind producers without receiving any moisture-attributed virtual water through trade, while $+1$ indicates structural dependence entirely on third-party atmospheric moisture transmitted through producing mediators before reaching the country via trade. Note that the analysis traces atmospheric moisture through network topology without quantifying how much of the precipitation volumes actually fall on the agricultural areas producing export commodities (i.e. we assume equal distribution within the moisture import country).

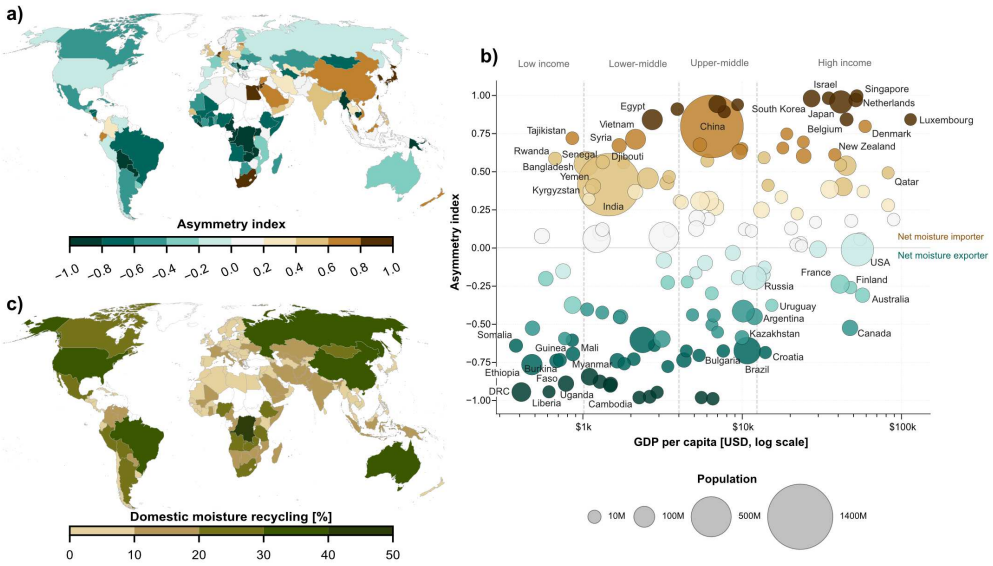


Fig. 3 Global patterns of moisture-to-trade asymmetry (a) Global distribution of the asymmetry index, representing the balance between a country's role as an atmospheric moisture source versus its reliance on VWT destinations. Teal regions indicate net moisture exporters (negative values), while brown regions indicate net moisture importers (positive values). **(b)** Relationship between the asymmetry index and economic development (GDP per capita, log scale). Bubbles are sized by population and coloured by their asymmetry index (matching panel **a**). Dashed vertical lines demarcate World Bank income groups (low ($< 1,015$\$), lower middle ($1,015$\$ $-$ $4,007$\$), upper middle ($4,007$\$ $-$ $12,371$\$), and high ($> 12,371$\$)). **(c)** Global distribution of the domestic moisture recycling (DMR) ratio, illustrating the fraction of a country's precipitation that originates from its own internal evaporation. Country outlines are based on Eurostat GISCO boundaries.

The global asymmetry index (Fig. 3a) reveals a clear spatial pattern in which countries are either net sources or net sinks of moisture-attributed virtual water flows, spanning from -0.99 (Serbia, Paraguay) to $+0.99$ (Singapore, Israel), with a global median of 0.07. Countries with strongly negative asymmetry, such as DRC, Bolivia, Paraguay, and Zambia, exhibit high domestic moisture recycling (DMR) yet import relatively low volumes of virtual water such that their atmospheric contribution outbalances their virtual water import. In countries with comparably high terrestrial moisture recycling but with larger virtual water import volumes, including China, the USA, Russia, and Bangladesh, the effect is offset toward symmetry or a net importer position. Strongly negative values are concentrated in central Africa, South America, and parts of Eastern Europe, while strongly positive values are concentrated in East Asia, the Middle East and North Africa, and several trade-intensive European economies. Arid or densely populated countries with large virtual water import volumes, among them Japan, South Korea, Israel, Egypt, and South Africa, record the highest asymmetry values (> 0.8), indicating strong dependence on third-party atmospheric moisture transmitted through a producing mediator before reaching

them via trade.

We further find that a wealth gradient underlies these geographic patterns (Fig. 3b). Wealthier countries, with few exceptions (e.g., Canada), tend to be net importers of moisture-attributed trade flows, while lower-income countries tend to be net exporters, as reflected in a positive correlation between GDP per capita and the asymmetry index (Pearson r = 0.42, $p < 0.001$). High-income countries average a net-importer position, with 77% on the positive side, while low-income countries average a net-exporter position (82%). This suggests a certain directionality in moisture-attributed flows, where atmospheric water recycled over lower-income regions tends to be embedded in trade flows directed toward wealthier nations. A subset of countries, including Bangladesh, Jordan, Tajikistan, and Rwanda, are identified as net importers despite low GDP per capita.

Across most countries, DMR (Fig. 3c) is modest (<30%), with a global maximum of approximately 40%, indicating that direct atmospheric self-sufficiency is the exception rather than the rule. This has direct bearing on the asymmetry patterns above, since a country's DMR sets an upper bound on how much of its atmospheric contribution originates from its own land surface, such that even strongly negative asymmetry countries remain dependent on foreign or oceanic evaporation for a substantial share of their precipitation.

Uneven global distribution of coupled exposure

Moisture-to-trade exposure captures a country's atmospheric moisture reliance that occurs upwind of its direct trading partners within the structural assumptions of the feed-forward triple framework; flows are traced purely based on the typology of the networks. Specifically, it measures the fraction of imported virtual water that can be attributed to atmospheric moisture originating from a third-party source region before reaching the destination through trade, making it a measure of how concentrated and how distant a country's atmospheric dependencies are. Globally, this exposure varies substantially, with a median of 0.20 and a range of 0.01 to 0.46 (Fig. 4a). A large part of the global network operates with limited redundancy in these pathways, with 29 countries reached through a single mediator and 70 through five or fewer (Fig. 4b), indicating that for many countries moisture-attributed trade flows are concentrated rather than distributed across alternative routes.

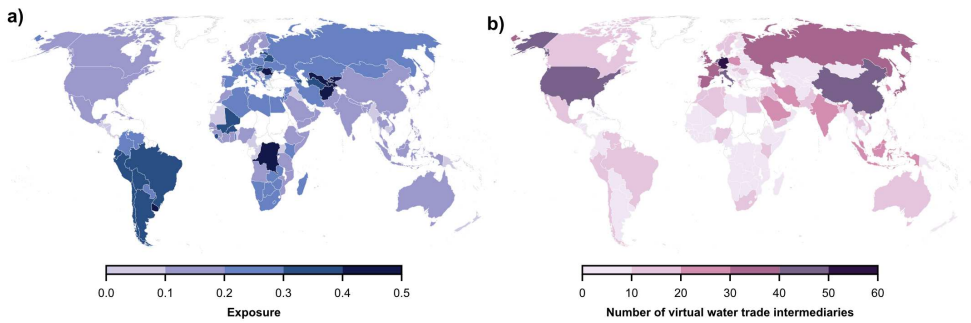


Fig. 4 Structural moisture-to-trade exposure and pathway redundancy. (a) Moisture-to-trade exposure, defined as the fraction of each country's total virtual water imports that can be structurally attributed to atmospheric moisture recycled over a foreign moisture source country, computed across all feed-forward triples. **(b)** Mediator redundancy, defined as the number of distinct mediator countries through which moisture-attributed virtual water flows reach each destination. Country outlines are based on Eurostat GISCO boundaries.

Japan (0.11), South Korea (0.12), and China (0.13) are among the least exposed countries globally (Fig. 4b) while being among the largest net receivers of moisture-attributed flows (Fig. 3a), and are supplied by 24 to 41 distinct intermediaries (Fig. 4a). Several countries in the Middle East and North Africa, including Lebanon (0.25), Syria (0.35), and Jordan (0.22), combine moderate exposure (Fig. 4b) with low mediator redundancy, supplied by only 5 to 12 mediator pathways (Fig. 4a). These countries are simultaneously net receivers of moisture-attributed trade flows (Fig. 3a), reliant on third-party atmospheric moisture for a substantial share of their imports, and supplied by a limited number of intermediaries. Unlike East Asian net receivers whose exposure is distributed, MENA net receivers face exposure that is concentrated and supported by few alternative supply routes.

South American countries such as Argentina (0.34), Brazil (0.35), and Uruguay (0.41) are among the most exposed countries, despite being net exporters of moisture-attributed trade (Fig. 3a). These countries contribute more atmospheric moisture to the network than is balanced through trade, yet the virtual water flows directed towards them are concentrated to a small number of specific atmospheric sources transmitted through few intermediaries (Fig. 3a). Their prominent role as moisture source co-occurs with a concentrated exposure to foreign moisture in VWT flows (Fig. 4b). Kazakhstan and Uzbekistan (0.29 and 0.45) present a similar case. European countries are generally near the mean in exposure (0.15 to 0.30) but are well-buffered by high mediator redundancy. Germany (55 intermediaries), Italy (45), and the United Kingdom (35) are supplied by the most diverse moisture pathway networks.

Moisture-to-trade flows routed through small set of intermediaries

To assess which countries function as critical mediators in the coupled system, we systematically remove each country from its mediator role by severing its incoming atmospheric moisture links ($\cdot \to b$) and outgoing trade links ($b \to \cdot$), and measure the resulting change of moisture-attributed flow across all $a \to b \to c$ triples. The resulting knockout volume reflects potential mediation capacity within the network topology. We use Sankey diagrams to illustrate which downstream countries receive the highest amount of trade-mediated moisture through a set of key mediators (Fig. 5).

Removing individual countries from the coupled moisture-trade network reveals pronounced asymmetries in systemic importance quantified by how much water each country mediates between atmospheric sources and trade destinations. Mediator knock-out effects are strongly skewed, indicating that a small set of producer–exporters route a large share of the global moisture-trade-coupling ($a \to b \to c$). The largest contribution of total flow occurred for Argentina (17%), United States (4.9%), Ukraine (4.9%), Belgium (4.8%), Côte d'Ivoire (4.7%), Canada (4.4%), Paraguay (3.8%), Kazakhstan (3.5%), Russia (3.5%), Malaysia (3.3%), Germany (3.2%), and Brazil (3.1%) (Fig. 5). Argentina is the single most critical mediator, contributing 47.3 km^3 of moisture-attributed VWT across all feed-forward triples, more than triple the contribution of the next ranked countries, the United States and Ukraine (13.9 km^3 and 13.8 km^3, respectively).

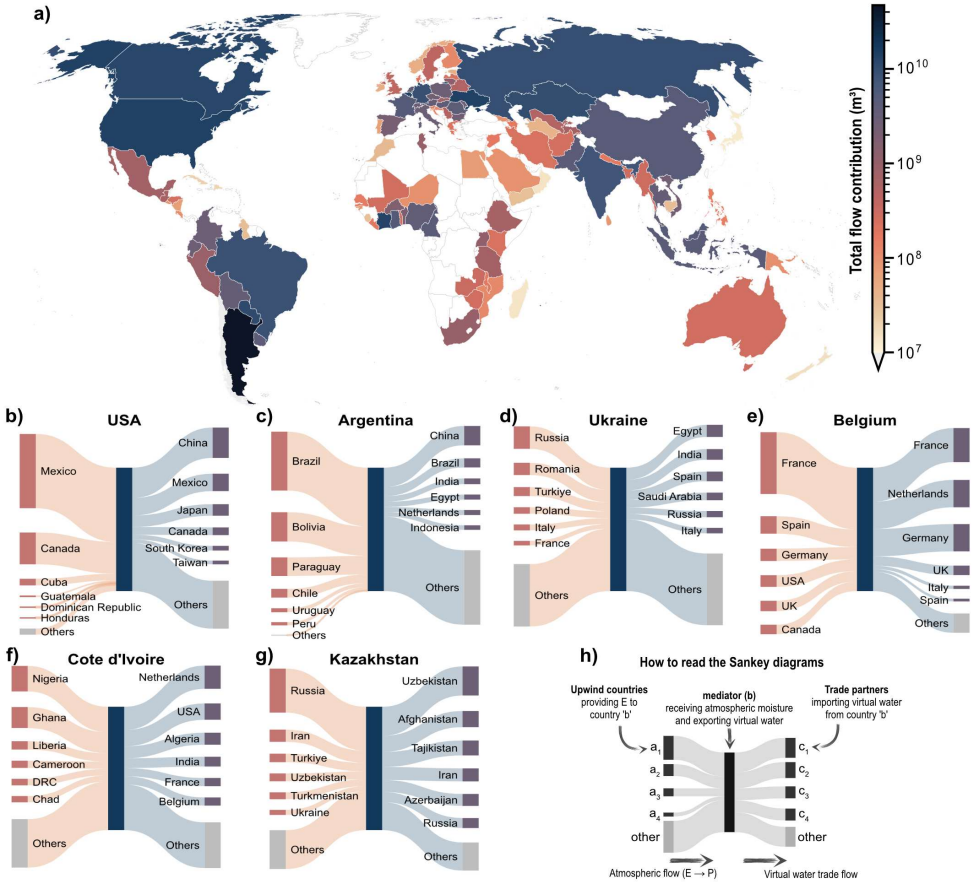


Fig. 5 Mediator knock-out effects and moisture-to-trade pathways of key mediator countries. (a) Total moisture-attributed VWT brokered (m^3) by each country in its mediator role in the coupled network (centre). Darker colours indicate higher mediation capacity, illustrating countries that act as critical conduits of moisture-attributed VWT. Country outlines are based on Eurostat GISCO boundaries. **(b - g)** Selected Sankey diagrams illustrate moisture-to-trade flow pathways for six countries within the top ten by total mediation capacity: United States **(b)**, Argentina **(c)**, Ukraine **(d)**, Belgium **(e)**, Côte d'Ivoire **(f)**, and Kazakhstan **(g)**, chosen to represent diverse geographical regions. Link width is proportional to the share of moisture received (orange) or virtual water exported (blue). Grey nodes indicate aggregated remaining countries. **(h)** Annotated guide to reading the Sankey diagrams.

Critical mediators differ both in the magnitude of redistributed flow and in the composition of their moisture sourcing and trade destinations. Key moisture sources are geographically-bound, tending to be neighbours of the mediator country (e.g, Brazil, Bolivia, and Paraguay supply to Argentina; Russia and Turkey supply to Ukraine; Mexico and Canada supply the US). On the destination side, the Netherlands, India, and Italy each appear across at least five of the top mediators, and

Belgium, China, France and Japan across four, suggesting that disruptions to any major conduit converge on the same set of import-dependent countries, several of which also act as re-export hubs supplying commodities further downstream. Mediation varies considerably across regions: the United States and Malaysia distribute trade flows broadly across many destinations, while Côte d'Ivoire draws moisture from a geographically concentrated set of West African neighbours yet exports broadly to Europe and North America, consistent with its role as a commodity exporter supplying distant high-income markets. China occupies a dual role, appearing as a moisture source for three of the top mediators and a trade destination for five. This reflects its simultaneous contribution to continental moisture recycling and its position as a dominant importer of embedded water.

Discussion and conclusion

By considering atmospheric and trade network layers jointly, we show that trade disruptions may be driven by transboundary exposure along an atmospheric moisture–production–trade pathway, meaning that imports depend not only on producing countries, but also on the moisture source regions that sustain production in those countries. Countries positioned as significant net sources of moisture-attributed flows include DRC, Bolivia, Paraguay, and Zambia, whose atmospheric contributions to the network outweigh the moisture-attributed virtual water that they import. Conversely, net sinks are concentrated in East Asia, the Middle East and North Africa, and trade-intensive European economies. These countries face a potential compound exposure: as net importers of moisture-attributed trade flows, they depend partly on their VWT, but also on the atmospheric moisture conditions of the source regions that support those exporters' water availability. A disruption at either node of this chain, whether a shift in moisture recycling in a source region or a breakdown in the trade relationship with the mediator, can propagate to the destination.

We further find a wealth gradient underlying these patterns, where lower-income countries tend to occupy the net-exporter position, while higher-income countries occupy the net-importer position, suggesting a directional global south to global north flow of appropriated atmospheric moisture embedded in traded commodities. Several high-income countries (Australia, Canada, and France) are net exporters, however: trade specialisation, agricultural production, and geographic factors likely modulate the relationship between wealth and moisture asymmetry. Bangladesh, Jordan, Tajikistan, Rwanda, and others, represent a subset of countries who are positioned as net receivers of moisture-attributed flows despite low GDP per capita, combining exposure to foreign atmospheric moisture and trade with potentially limited capacity to absorb or adapt to supply disruptions compared to higher-income countries.

Import-dependent countries face exposure not only to direct trade disruptions, but also to hydro-climatic variability beyond their visible supply chains, transmitted through a small set of critical intermediaries. Russia, Ukraine, and Kazakhstan - key

mediators in this study - supply ∼26% of global wheat exports, yet their combined exports collapsed from 33 to 11 million tonnes following the 2010 and 2012 droughts [30], contributing to a 23% wheat price spike and social instability across the MENA region [14]. Crucially, diversifying trade partners alone may not buffer this exposure. In South America, major exporters supply moisture to one another in a circular dependency, also described by Pranindita et al. (2025) [3], meaning perturbations such as Amazonian deforestation could reverberate simultaneously across the entire regional network. Effective risk reduction may therefore require attention to the stability of evaporation sources underpinning agricultural productivity across multiple exporters simultaneously. Most moisture-to-trade coupling is routed through Argentina (17%), the USA, Ukraine, and Paraguay, which act simultaneously as atmospheric moisture sinks and major agricultural exporters (Fig. 5), consistent with Pranindita et al. (2025)[3], who identify analogous patterns for forest-sourced moisture flows.

The results are based on topological and structural analyses that map the architecture of potential propagation pathways. A sensitivity analysis shows that key network metrics remain stable across flow volume thresholds, with substantial changes emerging only above 95% (Extended data, Fig. 8). The feed-forward representation is intentionally simple and does not quantify adaptive feedbacks (e.g., price responses, market substitution, irrigation expansion, export controls, crop switching) that may amplify or buffer cascades through the network. The full node removal scenarios are likewise an extreme counterfactual, as real disruptions - driven by hydro-climatic shocks, conflict, economic crises, or export restrictions [31, 32] - are typically partial and time-limited. Trade and moisture recycling patterns also vary year-to-year [33]; a time-resolved analysis would help distinguish chronic from episodic exposure [34, 35]. Sub-national or commodity-resolved trade analyses would allow more precise coupling for staple crops (e.g., maize, soy, wheat) [34, 36–38], better account for crop-specific water footprints [39, 40], and permit a more rigorous treatment of rain-fed versus irrigated agriculture, omitted here under the assumption that precipitation contributes meaningfully to crop water supply even in irrigated systems. Finally, the network metrics treat all countries equivalently regardless of size, which future analyses could address through area- and flow-weighted measures that scale network importance with country size and flow volume [21].

The increasing frequency of hydro-climatic shocks and climate changes poses a growing risk to agricultural productivity [41–43]. Crops are highly sensitive to weather and water extremes and variability [44], with significant decreases in productivity attributed to anomalously low precipitation events [45] and extreme heat [46], as well as smaller changes in mean annual precipitation [47]. While shocks are felt locally, their drivers may be remote, and in part driven by upwind countries' land management decisions [4, 48], including large-scale deforestation and irrigation [1, 49–51]. As land-use change and climate change alter atmospheric moisture flows, the coupled dependencies identified here may intensify, increasing risks for countries that rely on stable upwind evaporation to sustain both rainfall and food imports.

This study highlights that water resilience depends on both physical dependence on atmospheric moisture from neighbouring regions and on virtual water trade dependencies, revealing systemic vulnerabilities that cross hydrological and economic boundaries. This reflects a critical challenge in an era of an increasingly unstable hydrological cycle [10, 52] and increasing geopolitical fragmentation [53]. Understanding and monitoring both dimensions of this exposure is essential for meaningful water and food security governance [20, 54].

Methods

Overview

We analyse two directed, weighted global networks [55] defined over the same set of countries. The first is an atmospheric moisture transport network describing how terrestrial evaporation in one country contributes to precipitation in another. The second is a VWT network describing water embodied in traded agricultural commodities between exporter and importer countries. We then couple these networks in a three-step pathway that links an upwind moisture source country (a) to a mediator country (b) that receives precipitation, and onward to a downstream trade destination country (c). This coupling provides country-level measures of (i) whether a country is a net source or net sink of water within the moisture-to-trade pathways (asymmetry), (ii) how strongly a country's imports are linked to upwind moisture sources through supply chains (moisture-to-trade exposure), and (iii) which countries act as important mediators connecting the two layers.

Data and network construction

Both networks are defined on the same node set V of $n = 229$ countries. For each layer $\ell \in \{\text{atm}, \text{vwt}\}$ we define a directed weighted adjacency matrix:

$$W^{(\ell)} = \left[w_{ij}^{(\ell)}\right]_{i,j\in V}, \qquad w_{ij}^{(\ell)} \geq 0, \tag{1}$$

where $w_{ij}^{(\ell)}$ is the annual mean flow from country i to country j in layer ℓ. Self-loops are removed by setting $w_{ii}^{(\ell)} = 0$.

The atmospheric moisture network is taken from De Petrillo et al. (2025)[16] based on the UTrack dataset of atmospheric moisture trajectories, which contains mean monthly trajectories of evapotranspired water from source regions to precipitation sinks averaged over 2008 - 2017 [56]. De Petrillo et al. (2025)[16] aggregated the moisture flows at country- and ocean-scale and closed the global atmospheric water balance using an iterative proportional fitting algorithm. The VWT network is constructed from national water footprints of primary and processed crops for 2008–2016, taken from the CWASI database [27]. In both networks, edge weights represent the volumetric magnitude of water transfer (in m^3), and edges are directed from source to sink, from exporter to importer of atmospheric or virtual water.

To focus on the strongest connections, we apply the same percentile-based filter in each layer. Let $S^{(\ell)} = \{w_{ij}^{(\ell)} > 0\}$ be the multiset of non-zero edge weights and let $\tau_p^{(\ell)}$ be the p-th percentile of $S^{(\ell)}$ (here $p = 93$; see also Extended Data, Fig. 10). We set all weaker flows to zero:

$$\tilde{w}_{ij}^{(\ell)} = \begin{cases} w_{ij}^{(\ell)}, & \text{if } w_{ij}^{(\ell)} \geq \tau_p^{(\ell)}, \\ 0, & \text{otherwise.} \end{cases} \tag{2}$$

The resulting directed graphs include edge (i, j) if $\tilde{w}_{ij}^{(\ell)} > 0$.

The atmospheric network (Fig. 1a) is substantially larger than the VWT network (Fig. 1b), with total flows approximately 16 times higher and the largest individual link roughly 100 times greater. In terms of network connectivity, the atmospheric network is nearly fully connected (∼1.0), before thresholding, whereas the VWT network is more fragmented (∼0.6).

Single-layer flow roles

To provide descriptive context for the individual roles countries play within the separate AMF and VWT layers, we calculate four standard node-level network metrics: node-strength, in-strength, out-strength, and betweenness centrality. These metrics are computed on the filtered, directed adjacency matrices $\tilde{W}^{(\ell)}$ for each layer $\ell \in \{\text{atm}, \text{vwt}\}$.

The total volume of atmospheric moisture or virtual water entering and leaving a specific country i is quantified by the node in-strength (incoming flow) and out-strength (outgoing flow), respectively. These are defined as the sum of the filtered edge weights directed into and out of node i:

$$s_{i,\,\text{in}}^{(\ell)} = \sum_{j \in V} \tilde{w}_{ji}^{(\ell)} \qquad \text{(incoming flow to } i\text{)[57]}, \tag{3}$$

$$s_{i,\,\text{out}}^{(\ell)} = \sum_{j \in V} \tilde{w}_{ij}^{(\ell)} \qquad \text{(outgoing flow from } i\text{)[57]}. \tag{4}$$

In the atmospheric layer, high outflow identifies dominant upwind moisture source countries, while high inflow indicates major downwind precipitation sinks. In the VWT layer, these metrics correspond to total national import and export volumes of embodied water.

Node centrality measures were calculated to characterize the structural importance of countries within the networks. In weighted networks, node connectivity is captured by the weighted degree (node strength), which quantifies the total magnitude of flows connected to a node. For a node i, the weighted degree ($s_i^{(\ell)}$) is given by the sum of its in-strength and out-strength:

$$s_i^{(\ell)} = s_{i,\,\text{in}}^{(\ell)} + s_{i,\,\text{out}}^{(\ell)} \tag{5}$$

This measure captures the total magnitude of moisture or virtual water flows directly connected to each country, reflecting both the role of a country as a source and as a sink in the network.

In its unweighted form, degree centrality quantifies the number of direct connections of a node. For a node i in a network with N nodes, the normalized degree centrality is defined as

$$C_D(i) = \frac{k_i}{N-1} \tag{6}$$

where k_i is the count of all incoming and outgoing links connected to node i, regardless of their weight, and $N-1$ represents the maximum possible number of connections in a directed network [57].

To capture the role of countries as intermediaries in multi-step pathways, we computed weighted betweenness centrality. Betweenness centrality measures how frequently a node lies on shortest paths between pairs of other nodes and is defined as

$$C_B^{(\ell)}(i) = \sum_{\substack{s \neq i \\ t \neq i \\ s \neq t}} \frac{\sigma_{st}^{(\ell)}(i)}{\sigma_{st}^{(\ell)}} \tag{7}$$

where $\sigma_{st}^{(\ell)}$ denotes the total number of shortest paths between nodes s and t in layer l, and $\sigma_{st}^{(\ell)}(i)$ is the number of those paths that pass through node i [55]. Because the networks represent directed and weighted volumetric flows, shortest paths were computed using edge lengths defined as the inverse of the flow weight,

$$l_{ij}^{(\ell)} = \frac{1}{w_{ij}^{(\ell)}} \tag{8}$$

where $w_{ij}^{(\ell)}$ is the magnitude of the flow from node i to node j in layer ℓ. This transformation ensures that stronger connections correspond to shorter effective distances, such that high-volume pathways dominate shortest-path calculations. All network metrics were computed using the Python library NetworkX (v3.6.1) [58]. Corresponding results for in-strength and out-strength are presented in Extended Data Fig. 6, and degree centrality and betweenness centrality in Extended Data Fig. 7.

From individual networks to a coupled system

The core of the coupled analysis is the tripartite feed-forward pathway ($a \rightarrow b \rightarrow c$), representing the tele-coupling between terrestrial moisture sources (a), mediators (b) receiving precipitation and exporting goods, and virtual water destinations (c). The cross-network interactions are inferred by linking terrestrially-sourced precipitation to national crop production and subsequent trade flows (Fig. 1c). This approach

allows tracing how water originating in one country can indirectly support consumption in another, providing the basis for the coupled network analysis and subsequent evaluation of interdependencies.

To maintain physical interpretability and dimensional consistency, we utilize a volumetric attribution framework. We define the attributed coupled flow, F_{abc}, as the volume (m^3) of virtual water received in c that is physically sustained by terrestrial moisture originating in a. This is calculated by scaling the trade volume with the atmospheric moisture recycling ratio of the mediator:

$$F_{abc} = \left(\frac{W_{ab}^{(atm)}}{P_b} \right) \times W_{bc}^{(vwt)} \tag{9}$$

where P_b is the total annual precipitation in mediator b (m^3). This approach ensures that all coupled metrics represent absolute physical volumes of virtual water.

Functional asymmetry

First, we compare a country's role as a primary moisture source versus its role as a final virtual water sink. We define the total moisture-source volume ($V_{\text{source},i}$) and total trade-sink volume ($V_{\text{sink},i}$) as:

$$V_{\text{source},i} = \sum_{b,c} F_{ibc}, \qquad V_{\text{sink},i} = \sum_{a,b} F_{abi} \tag{10}$$

where $V_{\text{source},i}$ represents the total volume of moisture originating in country i that eventually could sustain downstream trade, and $V_{\text{sink},i}$ represents the total volume of virtual water imported by country i that is physically linked to tracked upwind moisture. The relative balance between these roles is captured by the asymmetry index (A_i):

$$A_i = \frac{V_{\text{sink},i} - V_{\text{source},i}}{V_{\text{sink},i} + V_{\text{source},i}} \tag{11}$$

where $A_i \in [-1, 1]$. A value of -1 identifies a pure source (contributing moisture but importing no moisture-linked trade), while $+1$ identifies a pure sink (relying on upwind moisture for imports without contributing to the atmospheric moisture supply of others). The asymmetry index reflects a countries' hydrological attribution in terms of two structural factors: a country's dependence on neighbouring countries evaporation (atmospheric moisture flow) and its integration within the global commodity trade system giving rise to moisture-attributed virtual trade dependencies.

Moisture-to-trade source and exposure

We quantify the potential exposure and impact of countries within the tripartite pathways by defining exposure and impact as normalized ratios of the coupled flow:

Coupled exposure (E_c): This represents the physical reliance of a destination country c on the tracked atmospheric moisture sources that sustain its trade portfolio. It is defined as the ratio of total moisture-attributed imports to the country's total virtual water import volume:

$$E_c = \frac{\sum_{a,b} F_{abc}}{\sum_j W_{jc}^{(\mathrm{vwt})}} \tag{12}$$

High exposure indicates that a significant portion of a country's food and commodity imports is sensitive to hydro-climatic changes in upwind moisture source regions.

Coupled source (S_a): Conversely, we measure the potential impact of a source country a by calculating the fraction of its terrestrial moisture export that successfully translates into global VWT. It is defined as:

$$S_a = \frac{\sum_{b,c} F_{abc}}{\sum_j W_{aj}^{(\mathrm{atm})}} \tag{13}$$

This metric identifies countries whose terrestrially recycled evaporation has the greatest systemic impact on the global trade of water-intensive commodities downwind.

Knock-out experiments and mediator effect

The tripartite structure ($a \to b \to c$) highlights the critical role of mediator countries (b) that act as the physical bridge between atmospheric moisture and global markets. To evaluate the systemic importance of these mediators, we perform *in-silico* knockout experiments.

In each simulation, a single mediator country b is removed from the system, effectively breaking all pathways that pass through that node. Because the coupled flow F_{abc} is mediated by the precipitation and production of country b, the resulting change in total coupled flow quantifies the moisture-attributed VWT that country b structurally contributes to the system by virtue of its mediator position in the network. The primary measure of a mediator's systemic importance is the **total flow contribution (ΔF_b)**, defined as the absolute volume (m^3) of moisture-attributed VWT brokered through node b across all feed-forward triples:

$$\Delta F_b = \sum_{a,c} F_{abc} \tag{14}$$

This knockout approach identifies "bottleneck" countries — mediators that are both major downwind recipients of moisture and major exporters of virtual water.

To further assess how this contribution is distributed geographically, we calculate the **relative mediator effect** at the destination level, representing the fraction of country c's total moisture-linked imports attributable to mediator b:

$$\tilde{F}_{b\to c} = \frac{\sum_a F_{abc}}{\sum_{a,k} F_{akc}} \tag{15}$$

This allows us to distinguish between mediators that are globally significant (high ΔF_b) and those that are locally critical for the supply-chain security of specific trading partners.

Additional data

To examine the relationship between a country's role and its economic development, we obtained data on the Gross Domestic Product (GDP) per capita (current US$) from the World Bank national accounts and OECD National Accounts data files [59], both are published under a CC BY-4.0 license. We calculated the average GDP per capita for each country across the study period (2008-2017) to ensure temporal consistency with the atmospheric and trade network datasets. Countries were categorized into income groups based on the World Bank's classification.

Data availability

All data used in this study are publicly available. VWT and water footprint data are obtained from the CWASI database [27, 60] and are available upon request via Zenodo (https://zenodo.org/doi/10.5281/zenodo.2643484). Atmospheric moisture flow data are derived from the country-ocean moisture flow dataset by [16, 61] and can be accessed via Zenodo (https://zenodo.org/doi/10.5281/zenodo.10400694). Economic data (GDP, *current US$*) are sourced from the World Development Indicators [59](https://data.worldbank.org/indicator/NY.GDP.MKTP.CD). Map geometries are based on Eurostat GISCO administrative boundary data (https://ec.europa.eu/eurostat/web/gisco/geodata/administrative-units/countries). The primary data generated in this study are available in a dedicated repository at: https://zenodo.org/records/19826335.

Code availability

The code used for this analysis is written in Python and is publicly available on GitHub at https://github.com/sifa4152/moisture_to_trade_pathways/releases/tag/v1.0.0 and in the Zenodo repository at https://zenodo.org/records/19826335. The repository includes input data, pre-processing scripts, network analysis code, and post-processing and plotting routines.

Acknowledgements. We gratefully acknowledge the European Regional Development Fund, the German Federal Ministry of Education and Research, and the Land Brandenburg for supporting this project by providing resources on the high-performance computer system at the Potsdam Institute for Climate Impact Research. S.F.F. and L.S.A. are part of the Planetary Boundaries Science Lab's research effort at the Potsdam Institute of Climate Impact Research (PIK). This study was funded

by the Grantham Foundation for the Protection of the Environment. R.L. acknowledges funding from the Formas project SAFER with grant number 2022-02089 . J.F.D. acknowledges financial support from the project "CZS Research Groups for Earth System Modelling" funded by the Carl-Zeiss-Stiftung. L.W.-E. is supported by funding from Formas - a Swedish Research Council for Sustainable Development (2022-02089, 2023-00310, 2023-00321).

Author contributions. S.F.F., L.S.A. and N.W. conceived the idea. S.F.F. designed the research, conducted the analysis, interpreted the results, designed the figures, and wrote and edited the manuscript. R.L. contributed to the analysis, interpreted the results, designed the figures, and wrote and edited the manuscript. D.G., J.F.D., M.T. and A.S. contributed to the idea and research design and edited the manuscript. All authors edited the manuscript. L.W.-E., J.R. and N.W. supervised the study.

Extended Data

Network metrics comparison

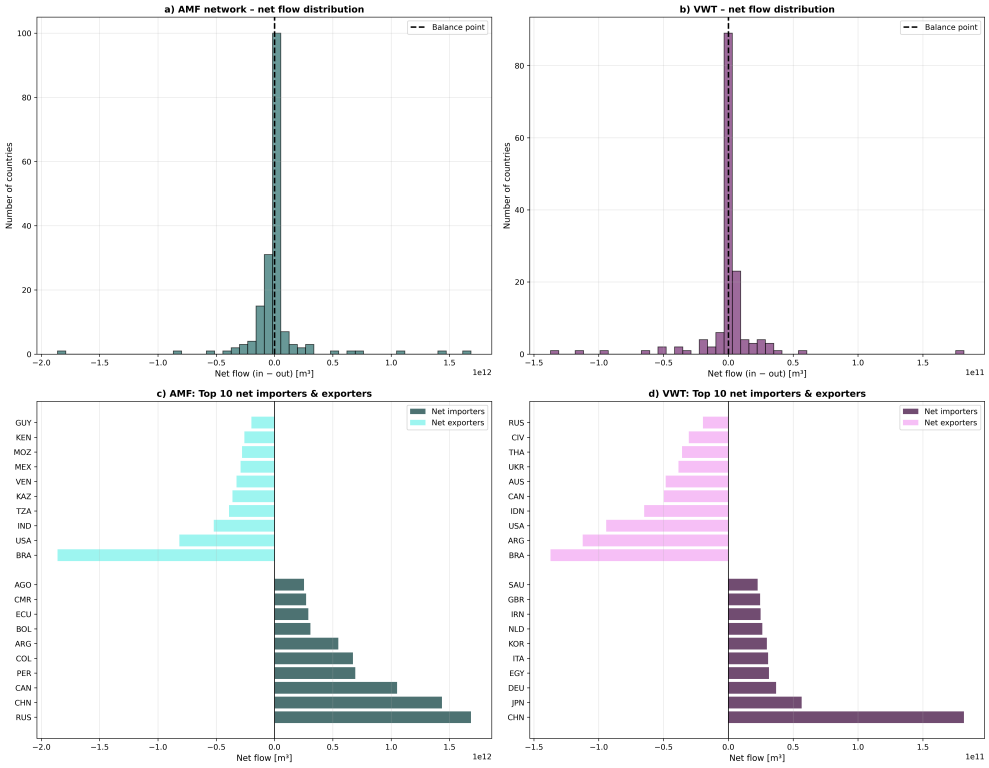


Fig. 6 Distributions of net flow (in-strength minus out-strength) and ranked net importers and exporters for the atmospheric moisture flow (AMF) and virtual water trade (VWT) networks. **(a)** Histogram of net flow across all active AMF network nodes. **(b)** Histogram of net flow across all active VWT network nodes. **(c)** Top 10 net importers and exporters in the AMF network, ranked by net flow magnitude. **(d)** Top 10 net importers and exporters in the VWT network, ranked by net flow magnitude. Country codes follow ISO 3166-1 alpha-3.

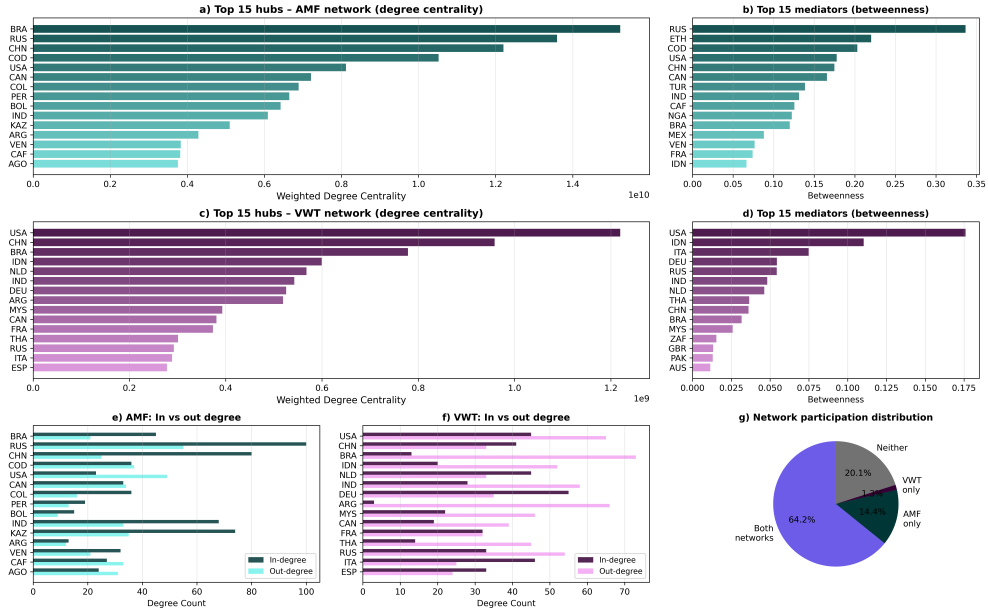


Fig. 7 Network centrality metrics histograms: Network centrality metrics for the top-ranked countries in the AMF (teal) and VWT (magenta) networks. **(a)** Top 15 countries by weighted degree centrality in the AMF network. **(b)** Top 15 countries by betweenness centrality in the AMF network. **(c)** Top 15 countries by weighted degree centrality in the VWT network. **(d)** Top 15 countries by betweenness centrality in the VWT network. **(e)** In- versus out-degree counts for the top 15 AMF hubs. **(f)** In- vs. out-degree counts for the top 15 VWT hubs. **(g)** Distribution of countries by network participation category (both networks, AMF only, VWT only, or neither). Country codes follow ISO 3166-1 alpha-3.

Threshold sensitivity analysis

To assess the robustness of the network metrics to the choice of flow volume threshold, we performed a sensitivity analysis varying the percentile cut-off used to filter edges in both networks from 0% to 99%. This was motivated by the need to confirm that key structural patterns, including asymmetry, exposure, and mediator rankings, are not artefacts of the filtering procedure. Network metrics remain stable across the full range of thresholds, with substantial changes emerging only above 95%, where network sparsity begins to affect connectivity (Fig. 8). The ranking of the top ten mediator countries is similarly robust across thresholds (Table 1).

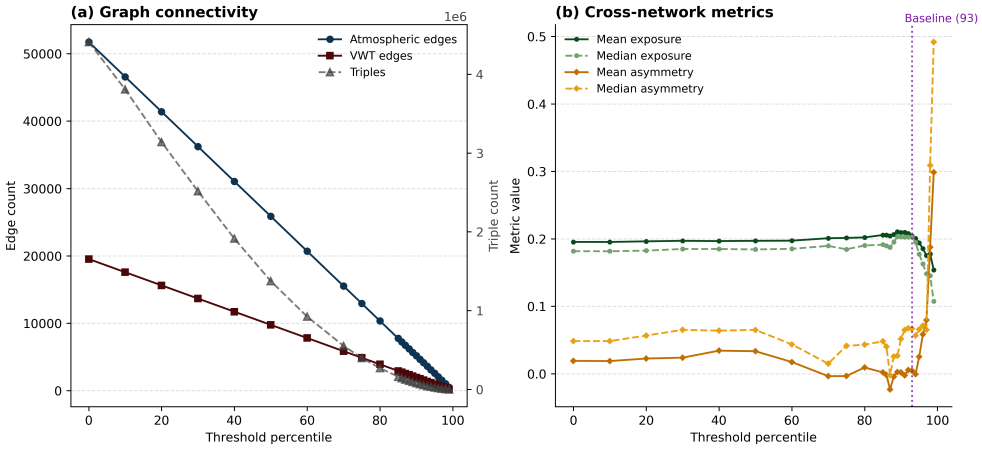


Fig. 8 Sensitivity analysis of network metrics to flow volume threshold. (a) Edge and triple counts across the atmospheric moisture network, virtual water trade network, and coupled feed-forward triples as a function of the flow percentile threshold applied to retain edges. **(b)** Mean and median values of moisture-to-trade exposure and asymmetry index across all countries as a function of the same threshold. The dotted vertical line indicates the baseline threshold of the 93rd percentile used in the main analysis.

Table 1 Sensitivity of mediator rankings to edge filtering threshold. Top ten mediator countries ranked by total flow contribution (ΔF_b) across percentile thresholds from 0% to 99%.

Threshold (%)	Top mediators
0	ARG, BEL, UKR, USA, CIV, CAN, PRY, KAZ, RUS, DEU
10	ARG, BEL, UKR, USA, CIV, CAN, PRY, KAZ, RUS, DEU
20	ARG, BEL, UKR, USA, CIV, CAN, PRY, KAZ, RUS, DEU
30	ARG, BEL, UKR, USA, CIV, CAN, PRY, KAZ, RUS, DEU
40	ARG, BEL, UKR, USA, CIV, CAN, PRY, KAZ, RUS, DEU
50	ARG, BEL, UKR, USA, CIV, CAN, PRY, KAZ, RUS, DEU
60	ARG, BEL, UKR, USA, CIV, CAN, PRY, KAZ, RUS, DEU
70	ARG, BEL, UKR, USA, CIV, CAN, PRY, KAZ, RUS, DEU
75	ARG, BEL, UKR, USA, CIV, CAN, PRY, KAZ, RUS, DEU
80	ARG, BEL, UKR, USA, CIV, CAN, PRY, KAZ, RUS, DEU
85	ARG, BEL, UKR, USA, CIV, CAN, PRY, KAZ, RUS, DEU
86	ARG, BEL, UKR, USA, CIV, CAN, PRY, KAZ, RUS, DEU
87	ARG, BEL, UKR, USA, CIV, CAN, PRY, KAZ, RUS, DEU
88	ARG, BEL, UKR, USA, CIV, CAN, PRY, KAZ, RUS, DEU
89	ARG, BEL, UKR, USA, CIV, CAN, PRY, KAZ, RUS, DEU
90	ARG, BEL, UKR, USA, CIV, CAN, PRY, KAZ, RUS, DEU
91	ARG, BEL, UKR, USA, CIV, CAN, PRY, KAZ, RUS, DEU
92	ARG, BEL, UKR, USA, CIV, CAN, PRY, KAZ, RUS, DEU
93	ARG, USA, UKR, BEL, CIV, CAN, PRY, KAZ, RUS, DEU
94	ARG, USA, UKR, CIV, BEL, CAN, PRY, RUS, KAZ, DEU
95	ARG, USA, UKR, CIV, CAN, BEL, KAZ, PRY, RUS, BRA
96	ARG, USA, UKR, CIV, CAN, KAZ, RUS, PRY, BRA, BEL
97	ARG, USA, CIV, UKR, CAN, KAZ, BRA, RUS, PRY, DEU
98	ARG, USA, CAN, CIV, UKR, KAZ, BRA, PRY, IND, RUS
99	ARG, USA, CAN, BRA, CIV, KAZ, IND, RUS, IDN, URY

References

[1] Keys, P. W. *et al.* Invisible water security: Moisture recycling and water resilience. *Water Security* **8**, 100046 (2019). URL https://www.sciencedirect.com/science/article/pii/S2468312419300057.

[2] Keys, P. W. & Wang-Erlandsson, L. On the social dynamics of moisture recycling. *Earth System Dynamics* **9**, 829–847 (2018).

[3] Pranindita, A., Teuling, A. J., Fetzer, I. & Wang-Erlandsson, L. Forests support global crop supply through atmospheric moisture transport. *Nature Water* **3**, 1243–1255 (2025). URL https://www.nature.com/articles/s44221-025-00518-4.

[4] Staal, A. *et al.* Forest-rainfall cascades buffer against drought across the Amazon. *Nature Climate Change* **8**, 539–543 (2018).

[5] van der Ent, R. J., Wang-Erlandsson, L., Keys, P. W. & Savenije, H. H. G. Contrasting roles of interception and transpiration in the hydrological cycle - Part 2: Moisture recycling. *Earth System Dynamics* **5**, 471–489 (2014). URL https://esd.copernicus.org/articles/5/471/2014/.

[6] Tuinenburg, O. A. & Staal, A. Tracking the global flows of atmospheric moisture and associated uncertainties. *Hydrology and Earth System Sciences* **24**, 2419–2435 (2020). URL https://hess.copernicus.org/articles/24/2419/2020/.

[7] Hoekstra, A. Y. & Hung, P. Q. Globalisation of water resources: international virtual water flows in relation to crop trade. *Global Environmental Change* **15**, 45–56 (2005). URL https://www.sciencedirect.com/science/article/pii/S0959378004000664.

[8] D'Odorico, P. *et al.* Global virtual water trade and the hydrological cycle: patterns, drivers, and socio-environmental impacts. *Environmental Research Letters* **14**, 053001 (2019). URL https://doi.org/10.1088/1748-9326/ab05f4.

[9] Konar, M. *et al.* Water for food: The global virtual water trade network. *Water Resources Research* **47** (2011). URL https://onlinelibrary.wiley.com/doi/abs/10.1029/2010WR010307.

[10] Porkka, M. *et al.* Notable shifts beyond pre-industrial streamflow and soil moisture conditions transgress the planetary boundary for freshwater change. *Nature Water* **2**, 262–273 (2024). URL https://www.nature.com/articles/s44221-024-00208-7.

[11] Samaniego, L. Permanent shifts in the global water cycle. *Science* **387**, 1348–1350 (2025). URL https://www.science.org/doi/10.1126/science.adw5851.

[12] Allen, J. A. Virtual water: a strategic resource. *Ground Water* **36** (1998).

[13] Burkholz, R. & Schweitzer, F. International crop trade networks: the impact of shocks and cascades. *Environmental Research Letters* **14**, 114013 (2019). URL https://doi.org/10.1088/1748-9326/ab4864.

[14] Bren d'Amour, C., Wenz, L., Kalkuhl, M., Christoph Steckel, J. & Creutzig, F. Teleconnected food supply shocks. *Environmental Research Letters* **11**, 035007 (2016). URL https://doi.org/10.1088/1748-9326/11/3/035007.

[15] Keys, P. W., Wang-Erlandsson, L., Gordon, L. J., Galaz, V. & Ebbesson, J. Approaching moisture recycling governance. *Global Environmental Change* **45**, 15–23 (2017).

[16] De Petrillo, E. *et al.* Reconciling tracked atmospheric water flows to close the global freshwater cycle. *Communications Earth & Environment* **6**, 347 (2025). URL https://www.nature.com/articles/s43247-025-02289-y.

[17] Tamea, S., Carr, J. A., Laio, F. & Ridolfi, L. Drivers of the virtual water trade. *Water Resources Research* **50**, 17–28 (2014). URL https://onlinelibrary.wiley.com/doi/abs/10.1002/2013WR014707. _eprint: https://agupubs.onlinelibrary.wiley.com/doi/pdf/10.1002/2013WR014707.

[18] Liu, J. *et al.* Framing Sustainability in a Telecoupled World. *Ecology and Society* **18** (2013).

[19] Cotta, B. *et al.* Environmental governance in globally telecoupled systems: Mapping the terrain towards an integrated research agenda. *Earth System Governance* **13**, 100142 (2022). URL https://www.sciencedirect.com/science/article/pii/S2589811622000118.

[20] Mekonnen, M. M. *et al.* Trends and environmental impacts of virtual water trade. *Nature Reviews Earth & Environment* **5**, 890–905 (2024). URL https://www.nature.com/articles/s43017-024-00605-2.

[21] Zemp, D. C., Wiedermann, M., Kurths, J., Rammig, A. & Donges, J. F. Node-weighted measures for complex networks with directed and weighted edges for studying continental moisture recycling. *Europhysics Letters* **107**, 58005 (2014). URL https://doi.org/10.1209/0295-5075/107/58005.

[22] Wunderling, N., Wolf, F., Tuinenburg, O. A. & Staal, A. Network motifs shape distinct functioning of Earth's moisture recycling hubs. *Nature Communications* **13**, 6574 (2022). URL https://www.nature.com/articles/s41467-022-34229-1.

[23] Boers, N. *et al.* Complex networks reveal global pattern of extreme-rainfall teleconnections. *Nature* **566**, 373–377 (2019). URL https://www.nature.com/articles/s41586-018-0872-x.

[24] Rosa, L., Chiarelli, D. D., Tu, C., Rulli, M. C. & D'Odorico, P. Global unsustainable virtual water flows in agricultural trade. *Environmental Research Letters* **14**, 114001 (2019). URL https://doi.org/10.1088/1748-9326/ab4bfc.

[25] Dalin, C., Wada, Y., Kastner, T. & Puma, M. J. Groundwater depletion embedded in international food trade. *Nature* **543**, 700–704 (2017). URL https://www.nature.com/articles/nature21403.

[26] Yin, C. *et al.* The dual impact of trade on the water–energy–food nexus globally. *Nature Sustainability* (2026). URL https://www.nature.com/articles/s41893-026-01796-w.

[27] Tamea, S., Tuninetti, M., Soligno, I. & Laio, F. Virtual water trade and water footprint of agricultural goods: the 1961–2016 CWASI database. *Earth System Science Data* **13**, 2025–2051 (2021). URL https://essd.copernicus.org/articles/13/2025/2021/.

[28] Dirmeyer, P. A., Brubaker, K. L. & DelSole, T. Import and export of atmospheric water vapor between nations. *Journal of Hydrology* **365**, 11–22 (2009). URL https://www.sciencedirect.com/science/article/pii/S0022169408005477.

[29] te Wierik, S. A., Gupta, J., Cammeraat, E. L. H. & Artzy-Randrup, Y. A. The need for green and atmospheric water governance. *WIREs Water* **7** (2019).

[30] Fellmann, T., Hélaine, S. & Nekhay, O. Harvest failures, temporary export restrictions and global food security: the example of limited grain exports from Russia, Ukraine and Kazakhstan. *Food Security* **6**, 727–742 (2014). URL https://doi.org/10.1007/s12571-014-0372-2.

[31] Organization, W. T. Food Prices and the Multiplier Effect of Export Policy. *WTO* (2012). URL https://www.wto-ilibrary.org/content/papers/25189808/127.

[32] Tamea, S., Laio, F. & Ridolfi, L. Global effects of local food-production crises: a virtual water perspective. *Scientific Reports* **6**, 18803 (2016). URL https://www.nature.com/articles/srep18803.

[33] Carr, J. A., D'Odorico, P., Laio, F. & Ridolfi, L. On the temporal variability of the virtual water network. *Geophysical Research Letters* **39** (2012). URL https://onlinelibrary.wiley.com/doi/abs/10.1029/2012GL051247.

[34] Fair, K. R., Bauch, C. T. & Anand, M. Dynamics of the Global Wheat Trade Network and Resilience to Shocks. *Scientific Reports* **7**, 7177 (2017). URL https://www.nature.com/articles/s41598-017-07202-y.

[35] Konar, M., Dalin, C., Hanasaki, N., Rinaldo, A. & Rodriguez-Iturbe, I. Temporal dynamics of blue and green virtual water trade networks. *Water Resources Research* **48** (2012). URL https://onlinelibrary.wiley.com/doi/abs/10.1029/2012WR011959.

[36] Wu, F. & Guclu, H. Global Maize Trade and Food Security: Implications from a Social Network Model. *Risk Analysis* **33**, 2168–2178 (2013). URL https://onlinelibrary.wiley.com/doi/abs/10.1111/risa.12064.

[37] Barigozzi, M., Fagiolo, G. & Garlaschelli, D. Multinetwork of international trade: A commodity-specific analysis. *Physical Review E* **81**, 046104 (2010). URL https://link.aps.org/doi/10.1103/PhysRevE.81.046104.

[38] Lathuillière, M. J. *et al.* International reliance on Brazil's water through soy and beef supply chains. *Communications Earth & Environment* **6**, 688 (2025). URL https://www.nature.com/articles/s43247-025-02658-7.

[39] Mialyk, O. *et al.* Water footprints and crop water use of 175 individual crops for 1990–2019 simulated with a global crop model. *Scientific Data* **11**, 206 (2024). URL https://www.nature.com/articles/s41597-024-03051-3.

[40] Mekonnen, M. M. & Hoekstra, A. Y. The green, blue and grey water footprint of crops and derived crop products. *Hydrology and Earth System Sciences* **15**, 1577–1600 (2011).

[41] Wheeler, T. & von Braun, J. Climate Change Impacts on Global Food Security. *Science* **341**, 508–513 (2013). URL https://www.science.org/doi/full/10.1126/science.1239402.

[42] Gornall, J. *et al.* Implications of climate change for agricultural productivity in the early twenty-first century. *Philosophical Transactions of the Royal Society B: Biological Sciences* **365**, 2973–2989 (2010). URL https://doi.org/10.1098/rstb.2010.0158.

[43] Tigchelaar, M., Battisti, D. S., Naylor, R. L. & Ray, D. K. Future warming increases probability of globally synchronized maize production shocks. *Proceedings of the National Academy of Sciences* **115**, 6644–6649 (2018).

[44] Ray, D. K., Gerber, J. S., MacDonald, G. K. & West, P. C. Climate variation explains a third of global crop yield variability. *Nature Communications* **6**, 5989 (2015). URL https://www.nature.com/articles/ncomms6989.

[45] Sivakumar, M. V. K., Das, H. P. & Brunini, O. Impacts of Present and Future Climate Variability and Change on Agriculture and Forestry in the Arid and Semi-Arid Tropics. *Climatic Change* **70**, 31–72 (2005). URL https://doi.org/10.1007/s10584-005-5937-9.

[46] Battisti, D. S. & Naylor, R. L. Historical Warnings of Future Food Insecurity with Unprecedented Seasonal Heat. *Science* **323**, 240–244 (2009). URL https://www.science.org/doi/full/10.1126/science.1164363.

[47] Lobell, D. B. & Burke, M. B. Why are agricultural impacts of climate change so uncertain? The importance of temperature relative to precipitation. *Environmental Research Letters* **3**, 034007 (2008). URL https://doi.org/10.1088/1748-9326/3/3/034007.

[48] Pranindita, A., Wang-Erlandsson, L., Fetzer, I. & Teuling, A. J. Moisture recycling and the potential role of forests as moisture source during European heatwaves. *Climate Dynamics* **58**, 609–624 (2022). URL https://doi.org/10.1007/s00382-021-05921-7.

[49] Wang-Erlandsson, L. *et al.* Remote land use impacts on river flows through atmospheric teleconnections. *Hydrology and Earth System Sciences* **22**, 4311–4328 (2018).

[50] Alves, L. M., Marengo, J. A., Fu, R. & Bombardi, R. J. Sensitivity of Amazon Regional Climate to Deforestation. *American Journal of Climate Change* **06**, 75–98 (2017). URL http://www.scirp.org/journal/doi.aspx?DOI=10.4236/ajcc.2017.61005.

[51] Spera, S. A., Galford, G. L., Coe, M. T., Macedo, M. N. & Mustard, J. F. Land-use change affects water recycling in Brazil's last agricultural frontier. *Global*

Change Biology **22**, 3405–3413 (2016). URL https://onlinelibrary.wiley.com/doi/abs/10.1111/gcb.13298.

[52] Rodell, M. & Li, B. Changing intensity of hydroclimatic extreme events revealed by GRACE and GRACE-FO. *Nature Water* **1**, 241–248 (2023). URL https://www.nature.com/articles/s44221-023-00040-5.

[53] Aiyar, S. *et al.* Geo-Economic Fragmentation and the Future of Multilateralism. *Staff Discussion Notes* **2023**, 1 (2023). URL https://elibrary.imf.org/openurl?genre=journal&issn=2617-6750&volume=2023&issue=001.

[54] King, R. The water footprints of global food and agriculture trade: Why the 'virtual water' use hidden in supply chains is critical to sustainability. Tech. Rep., Royal Institute of International Affairs (2025). URL https://www.chathamhouse.org/2025/12/water-footprints-global-food-and-agriculture-trade.

[55] Newman, M. *Networks* 2 edn (Oxford University Press, Oxford, 2018).

[56] Tuinenburg, O. A., Theeuwen, J. J. E. & Staal, A. High-resolution global atmospheric moisture connections from evaporation to precipitation. *Earth System Science Data* **12**, 3177–3188 (2020). URL https://essd.copernicus.org/articles/12/3177/2020/.

[57] Barabási, A.-L. & Pósfai, M. *Network science* (Cambridge University Press, Cambridge, 2016).

[58] Hagberg, A. A., Schult, D. A. & Swart, P. J. Varoquaux, G., Vaught, T. & Millman, J. (eds) *Exploring network structure, dynamics, and function using networkx.* (eds Varoquaux, G., Vaught, T. & Millman, J.) *Proceedings of the 7th Python in Science Conference (SciPy 2008)*, 11–15 (Pasadena, California, 2008).

[59] Bank, W. GDP (current US$) (2026). URL https://data.worldbank.org/indicator/NY.GDP.MKTP.CD. Indicator: NY.GDP.MKTP.CD.

[60] Tamea, S. *et al.* CWASI database: virtual water trade and water footprint of agricultural products (1961-2023) (2026). URL https://zenodo.org/doi/10.5281/zenodo.2643484.

[61] De Petrillo, E. *et al.* Country-ocean-moisture-flows-reconciled-with-ERA5-reanalysis obtained processing Lagrangian moisture connections (2026). URL https://zenodo.org/doi/10.5281/zenodo.10400694. ISSN: 2662-4435.